



MiR-875-5p inhibits hepatocellular carcinoma cell proliferation and migration by repressing *astrocyte elevated gene-1 (AEG-1)* expression

Caixia Hu¹, Shichang Cui¹, Jiasheng Zheng¹, Tian Yin¹, Junsheng Lv², Jiang Long¹, Wenwen Zhang³, Xun Wang³, Shoupeng Sheng¹, Honghai Zhang¹, Yu Sun¹, Hongguang Wang³, Cong Li^{1,4,5,6}

¹Center of Oncology and Minimally Invasive Intervention, Beijing You-an Hospital, Capital Medical University, Beijing 100069, China; ²Department of General Surgery, Beijing Shunyi Hospital, Capital Medical University, Beijing 101300, China; ³Department of Hematological Surgery, General Hospital of Chinese PLA, Beijing 100853, China; ⁴Department of General Surgery, Beijing You-an Hospital, Capital Medical University, Beijing 100069, China; ⁵Department of Surgery ICU, ⁶Department of Surgery for Teaching and Research Section, General Hospital of Chinese PLA, Beijing 100853, China

Contributions: (I) Conception and design: C Li; (II) Administrative support: J Zheng; (III) Provision of study materials or patients: J Long; (IV) Collection and assembly of data: S Cui; (V) Data analysis and interpretation: C Hu; (VI) Manuscript writing: All authors; (VII) Final approval of manuscript: All authors.

Correspondence to: Cong Li. Center of Oncology and Minimally Invasive Intervention, Beijing You-an Hospital, Capital Medical University, Beijing 100069, China. Email: drcongli19850102@126.com; Hongguang Wang. Department of Hepatological Surgery, General Hospital of Chinese PLA, Beijing 100853, China. Email: wanghongguang301@163.com.

Background: Liver cancer or hepatocellular carcinoma (HCC) is one of the prevalent cancers with high mortality rate. There is no effective treatment for patients with unresectable HCC and approach for preventing metastasis.

Methods: The expression of miR-875-5p in HCC clinical samples was quantified by quantitative real-time polymerase chain reaction (qRT-PCR). The effects of miR-875-5p or *astrocyte elevated gene-1 (AEG-1)* on cancer cell migration and invasion were performed by transwell assay. The cell cycle analysis was performed by FACS. Luciferase-reporter assay showed that miR-875-5p targets the 3'-untranslated region (3'-UTR) of *AEG-1* to negatively regulate *AEG-1* expression.

Results: In this study, we found miR-875-5p, a potential tumor suppressing miRNA reported recently, was significantly decreased in HCC tissues. Overexpression of miR-875-5p inhibited cell migration, invasion, EMT progression and angiogenesis. In addition, miR-875-5p regulated *AEG-1* by directly binding to its 3'-UTR. In clinical samples of HCC, miR-875-5p was inversely correlated with *AEG-1*, which was upregulated in HCC. Deficiency of *AEG-1* expression partially suppressed the migration, invasion, EMT progression and angiogenesis in MHCC97-H cell line.

Conclusions: Taken together, these results elucidate the functions of miR-875-5p and its targets *AEG-1* in HCC, not only broadening our understanding of them in HCC development, but also suggesting their therapeutic potential in HCC treatment.

Keywords: Hepatocellular carcinoma (HCC); miRNA; metastasis; astrocyte elevated gene-1 (AEG-1); cancer therapy

Submitted Nov 08, 2017. Accepted for publication Jan 18, 2018.

doi: 10.21037/tcr.2018.01.22

View this article at: <http://dx.doi.org/10.21037/tcr.2018.01.22>

Introduction

Liver cancer or hepatocellular carcinoma (HCC) is the second highest worldwide cancer with high mortality rate but limited therapeutic options (1,2). HCC is influenced by various factors, including hepatitis B virus (HBV), hepatitis C virus (HCV), alcohol and nonalcoholic fatty liver disease (NAFLD) (3,4). However, the pathogenesis of HCC is not yet completely known.

Metastasis is the typical characteristics of cancers, consisting of tumor invasion, tumor cell dissemination, colonization of distant organs and metastatic outgrowth, which is one of the greatest challenges for cancer therapy (5). Effective prevention of metastasis would be the critical step for cancer therapy and prolonging lifespan. However, until now we still lack effective clinical therapy to inhibit metastasis (6).

Astrocyte elevated gene-1 (AEG-1), also known as metadherin (MTDH) has been reported to play a key role in the progression, invasion and metastasis of multiple human cancers. *AEG-1* overexpression in HCC cells increases the production of angiogenic factors, such as vascular endothelial growth factor (VEGF), placental growth factor, and fibroblast growth factor α . However, the regulatory mechanism is unclear (7).

MicroRNAs are small noncoding RNAs with approximately 19–25 nucleotides in length, which can bind to the 3'-untranslated region (3'-UTR) of target genes. The binding of miRNAs with the target genes 3'-UTRs results in the cleavage of target mRNAs or inhibiting protein translation, and negatively regulates the expression of target genes (8). Increasing number of reports have shown that miRNAs are involved in many biological processes, including cell proliferation, differentiation, metastasis, apoptosis and immune responses (9). MiR-21 promotes the growth of the breast cancer cell line MCF-7 both *in vitro* and *in vivo* (10). MiR-126 restoration reduces the growth and proliferation of tumors, and miR-335 inhibits metastatic cell invasion (11). MiR-29 is proved to inhibit metastasis through the targeting of TET1 in HCC carcinogenesis and progression (12). MiR-125a-5p inhibits cell proliferation and induces apoptosis in HBV-related HCC by down-regulation of ErbB3 (13).

Although substantial efforts have been made to identify miRNA functions, the molecular mechanism of miRNAs in tumorigenesis and metastasis is still not well understood.

MiR-875-5p as a novel microRNA reported recently is found to be down-regulated in prostate cancer tissues,

which impairs metastasis in prostate cancer models by repressing epithelial-mesenchymal transition (EMT) and enhances radiation response of prostate cancer cells via EGFR suppression (14). In addition, miR-875-5p works as a tumor suppressor by the down-regulation of EGFR in colorectal carcinoma (15). These results suggest the tumor-suppressive function of miR-875-5p and its role as an attractive target candidate for cancer therapy.

At present, the reports of miR-875-5p are limited and the role of miR-875-5p in HCC still remains ambiguous. Elucidation of miR-875-5p function in HCC and identification of its direct target may promote the development of HCC therapy. In the present study, we investigated the effects of miR-875-5p on MHCC97H cells by targeting *AEG-1*. Our data revealed that miR-875-5p is down-regulated in the HCC tissues compared with the matching paracarcinoma tissues (that is the matched adjacent non-cancer tissues). We also confirmed that miR-875-5p negatively regulates cell proliferation, migration, invasion and angiogenesis by targeting *AEG-1 in vitro*. These data revealed the underlying mechanism by which miR-875-5p inhibited the migration and invasion of HCC and regard miR-875-5p as a novel prognostic biomarker for HCC patients.

Methods

Patient samples and cell line

Informed consent was obtained from all the patients and the present study was approved by the Ethics Committee of the Capital Medical University in accordance with the Declaration of General hospital of Chinese PLA. Samples (including 29 pairs of HCC and the corresponding adjacent normal tissues) were collected from hepatoma patients undergoing partial hepatectomy. The hepatoma cell lines MHCC97-H was cultured and maintained in Dulbecco's Modified Eagle's Medium containing 10% fetal bovine serum (FBS, Gibco, USA), 100 U/mL penicillin and 0.1 mg/mL streptomycin at 37 °C with 5% CO₂.

Plasmids, miRNA, siRNA and transient transfection

The 3'-UTR or the mutant 3'-UTR of *AEG-1* was cloned into the luciferase reporter vector to construct the plasmids pLUC-*AEG-1* and pLUC-mut-*AEG-1*. The miR-875-5p mimics, siRNAs of *AEG-1* and their negative controls (NC) were purchased from Ribo Biotech (Guangzhou, China).

The sequences of primers used are described as followings: shAEG: AAAAGCCATCTGTAATCTTATCACTCGAG TGATAAGATTACAGATGGC. Transient transfection was performed using Lipofectamine 2000 (Invitrogen, Carlsbad, CA, USA) according to the manufacturer's instructions.

RNA extraction and qRT-PCR

For clinical samples and cultured cell lines, total RNA was extracted by Trizol (Tiangen Biotech, Beijing, China) according to the manufacturer's protocols. The expression level of miR-875-5p was determined by qRT-PCR using the SYBR Premix Ex Taq Kit (Takara, Japan) in a DNA Engine Opticon2 system (Bio-Rad, USA). Primers were bought from Ribo Biotech. The steps for amplification were: denaturation at 95 °C for 3 min, amplification for 40 cycles at 95 °C for 12 s and 62 °C for 40 s. The melting curve was plotted from 62 to 95 °C, and read every 0.2 °C with a 2 s' hold). The U6 small nuclear RNA was used as an internal control. The results were calculated by the $2^{-\Delta\Delta CT}$ method and represented as fold changes.

Transwell migration and invasion assay

For migration assay, MHCC97-H cells were seeded into the upper chamber of a transwell insert (pore size 8 μ m, Costar) in 100 μ L of serum-free medium. Medium of 600 μ L containing 10% FBS was added in the lower chamber to act as a chemoattractant. Unmigrated cells were removed from the upper chamber by scraping with a cotton bud. The cells on the lower surface of the insert were fixed with 4% formaldehyde (Sigma, USA) and stained by crystal violet. For invasion assay, the upper chamber was coated by matrigel (BD, USA) according to the manufacturer's instructions. Cells were seeded into the matrigel-coated chamber and cultured for about 48 h. The next steps were as same as the migration assay.

Immunofluorescence

MHCC97-H cells cultured on cover slides in 24-well plates were transfected with miR-875-5p mimics, siRNA of AEG-1 and their NCs. After 48 h of culture, the cells were fixed with 4% formaldehyde, permeabilized with 0.1% Triton X-100 and blocked with 2% bovine serum albumin (BSA, Sigma, USA) for 1 h at room temperature. Then the cells were incubated with the primary antibodies E-cadherin and Vimentin (Abcam, USA) overnight, respectively.

Subsequently, the secondary antibodies conjugated with Alexa Fluor 488 were applied. Cell nucleus was stained with DAPI (Roche, USA). The cells were visualized using a fluorescence microscope (Nikon, Japan).

Cell proliferation assay

MHCC97-H cells were seeded into a 96-well plate at a density of 5×10^3 cells/well. Next day, the cells were transfected with the indicated miRNAs or siRNAs. About 72 h after transfection, the cells were incubated with 10% CCK8 reagent (Dojindo, Japan) for 1 h at 37 °C. The result was detected by the automatic spectrometer (EnSpire Multimode Plate Reader, Perkin Elmer, USA) at 450 nm.

Cell cycle analysis

Cells cultured in 6-well plates were transfected with the indicated miRNAs or siRNAs. After 48 h, the cells were collected and fixed in 70% ethanol at 4 °C for 2 h. The cells were then washed and resuspended in 100 mL phosphate-buffered saline (PBS). RNase (50 mg/mL) was added for RNA removal at 37 °C for 30 min. The cells were stained with 200 mL propidium iodide (PI) solution (KeyGen Biotech, Nanjing, China) at 4 °C for 30 min before analyzing using a FACS Aria cell sorting system (BD Biosciences, San Jose, CA, USA).

HUVEC tube formation assay

HUVEC cells were seeded in a 96-well matrigel-coated plate at a density of 3×10^4 cells/well. miRNA/siRNA or NC were transfected into MHCC97-H cells. The supernatants were collected at 72 h after transfection to add to the HUVEC cells, respectively. The tubule elongation and branching formation were analyzed afterwards. Visualize the cells using a light microscope. Take pictures of the images of the capillary network and count the tube lengths using the Scion image software. Visualize the cells using the light microscope. Take pictures of images of the capillary network and count the tube lengths and branches using the scion image software.

Luciferase assay

The reporter plasmid pLUC-AEG-1 or pLUC-mut-AEG-1 was transfected into MHCC97-H cells with miR-875-5p mimics or the NC. After 24 h of culture, luciferase assays were performed. At least three independent experiments

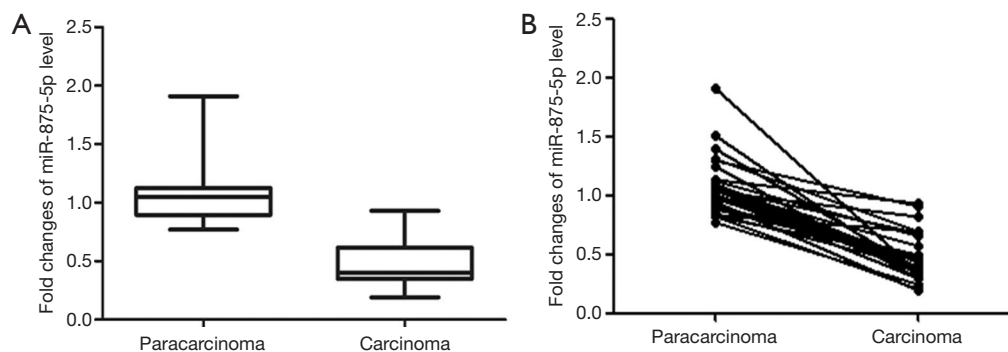


Figure 1 The expression of miR-875-5p in hepatocellular carcinoma tissues determined by qRT-PCR. (A) Box-plot of the data revealed that the mean level of miR-875-5p expression in carcinoma was significantly lower than that in matched adjacent non-cancer tissues (n=29, $P < 0.01$); (B) pair-wise comparison of miR-875-5p expression in carcinoma and the corresponding adjacent normal tissues. qRT-PCR, quantitative real-time polymerase chain reaction.

were performed.

Western blot analysis

After 48 h of transfection with the indicated miRNAs and siRNAs, the MHCC97-H cells were harvested for protein extraction. Proteins in lysates were separated by 10% sodium dodecyl sulfate polyacrylamide gel electrophoresis (SDS-PAGE) and then electrophoretically transferred to polyvinylidene fluoride (PVDF) membranes. After blocking, the membranes were incubated with the primary antibody (mouse anti-AEG-1, Protein Tech, Chicago, IL, USA) at 4 °C overnight and then with the secondary antibody (goat anti-mouse IgG-HRP, Santa Cruz, CA, USA) at room temperature for 1 h. Band signals were visualized using an enhanced chemiluminescence kit (Pierce, Minneapolis, MN, USA). β -actin (Santa Cruz, CA, USA) was used as the loading control.

Immunohistochemistry

Tumor samples were fixed in 10% buffered formalin, transferred to 70% ethanol and then embedded in paraffin. The paraffin lumps were sectioned and mounted on glass slides. Immunohistochemistry was performed using AEG-1 primary antibody at 4 °C overnight and then with the secondary antibody (goat anti-mouse IgG-HRP) followed by DAB staining.

Statistical analysis

All results were expressed as mean \pm SD derived from at

least three independent experiments. Statistical comparisons were made using an unpaired two-tailed student *t*-test. A *P* value < 0.05 was considered as significant. * indicates $P < 0.05$; ** indicates $P < 0.01$.

Results

Decreased expression of miR-875-5p in HCC tissues

The qRT-PCR method was performed to determine the expression levels of miR-875-5p in carcinoma tissues and matched adjacent non-cancer tissues. As shown in *Figure 1A*, the expression levels of miR-875-5p in HCC tissues was significantly decreased compared with those in the matched adjacent non-cancer tissues (29 pairs, $P < 0.01$). Pair-wise comparison also indicated that the expression level of miR-875-5p in carcinoma tissues was much lower than the corresponding adjacent normal tissues (*Figure 1B*).

MiR-875-5p inhibits metastatic traits in HCC cells

To explore the possible role of miR-875-5p in HCC cells, we first identified the effects of miR-875-5p on cancer cell migration and invasion by transwell assay. MiR-875-5p was overexpressed by transfection with miR-875-5p mimics in MHCC97-H cells indicated in *Figure S1*. As shown in *Figure 2A,B*, overexpression of miR-875-5p decreased the migratory ability of the cells with about 65% reduction compared to the NC. Similarly, the invasive capability of the cells was also significantly attenuated by 75%. EMT is the early event in tumor invasion and metastasis. Here, immunofluorescence

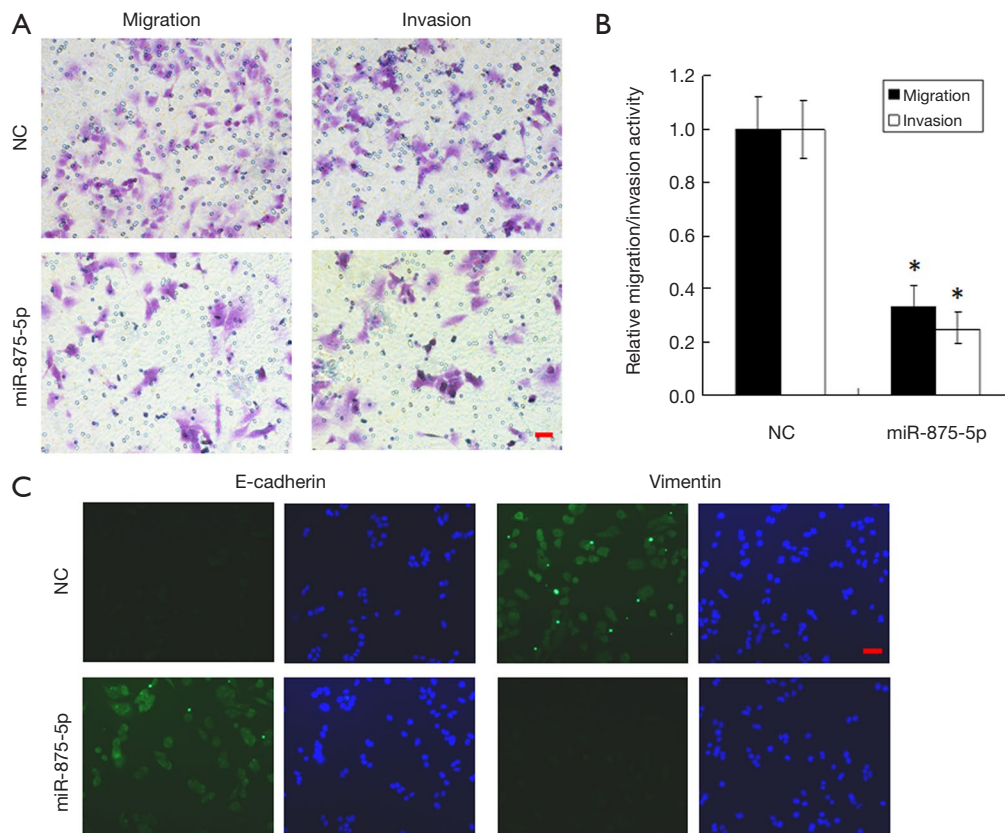


Figure 2 MiR-875-5p modulates metastatic traits in MHCC97-H cells. (A) Cell migration and invasion as assessed by transwell assays were inhibited by overexpression of miR-875-5p in MHCC97-H cells. The crystal violet staining for the migratory and invasive cells was assessed after miR-875-5p mimics and the NC transfection. The relative migration/invasion activity was shown in (B). Bar = 50 μ m. (C) Immunofluorescence for the expression of two EMT markers was analyzed after miR-875-5p mimics transfection. MHCC97-H cells were stained for E-cadherin (green) and Vimentin (green) respectively and DAPI for visualization of the nucleus (blue). The representative staining shows a 40 \times magnification. Bar = 100 μ m. * indicates $P < 0.05$; NC, negative control; EMT, epithelial-mesenchymal transition; DAPI, 2-(4-Amidinophenyl)-6-indolecarbamidine dihydrochloride.

analysis indicated that transfection of miR-875-5p mimics induced the up-regulated expression of an epithelial marker (E-cadherin) and the reduced expression of a mesenchymal marker (Vimentin), respectively (Figure 2C). The experiments were also performed in the HUH7 cells (Figure S2). In addition, another EMT marker *snai1* expression was obviously reduced in miR-875-5p-overexpressed cells as determined by qRT-PCR (Figure S3). These results demonstrate that miR-875-5p inhibits metastatic traits in HCC cells.

The effects of miR-875-5p on cell proliferation and cell cycle of HCC cells

To further identify the role of miR-875-5p, we analyzed

its effects on cell proliferation and cell cycle. The results showed that overexpression of miR-875-5p suppressed the cell proliferation by approximately 30% (Figure 3A). The change of cell proliferation is often due to the variation of cell cycle. Therefore, cell cycle analysis was performed by FACS after miR-875-5p transfection, showing the increased proportion of the cells in G1 phase but decreased proportion in G2/M phase compared with the control (Figure 3B). These findings indicate that miR-875-5p negatively regulates cell proliferation of HCC cells.

MiR-875-5p inhibits angiogenesis modeled by HUVEC cells in vitro

To investigate whether miR-875-5p has effects on

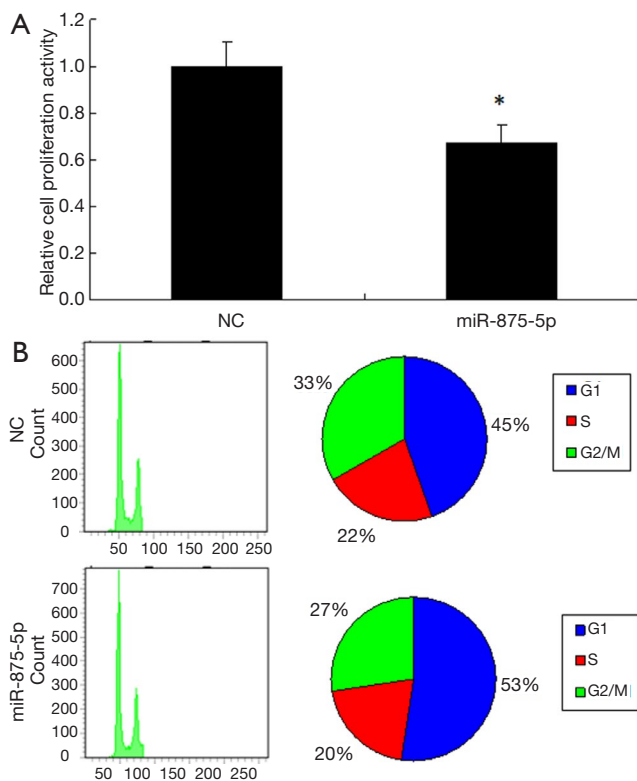


Figure 3 MiR-875-5p expression has effects on MHCC97-H cells proliferation. MiR-875-5p slightly induced G1 arrest and inhibits growth in MHCC97-H cells. (A) The viable cells were detected by CCK-8 assay 48 h after transfection with miR-875-5p mimics and NC; (B) MHCC97-H cells were transfected with miR-875-5p mimics and NC. The cells were collected and used for cell cycle analysis 48h post transfection by flow cytometry after PI staining. The peak on the left indicates cells have diploid DNA content, the peak on the right indicates cells have tetraploid DNA content. *, indicates $P < 0.05$. NC, negative control.

angiogenesis, we collected the supernatant 72 h after miR-875-5p mimic control transfected into MHCC97-H cells to add to the HUVEC cells, respectively. HUVEC cells were seeded onto the matrigel-coated plates without angiogenic stimuli in advance. The tubule elongation and branching formation were analyzed 2 days culture afterwards. Visualize the cells using a light microscope. Take pictures of the images of the capillary network and count the tube lengths using the Scion image software. As shown in *Figure 4*, miR875-5p over-expression significantly inhibited branching formation and tubule elongation compared to control.

MiR-875-5p targets the 3'-UTR of AEG-1 to reduce AEG-1 expression

To explore the molecular mechanism of miR-875-5p, we predicted the possible target gene of miR-875-5p using the miRNA.org algorithm. As shown in *Figure 5A*, the binding of miR-875-5p with the 3'-UTR of *AEG-1* was predicted, suggesting that *AEG-1* gene may be a target of miR-875-5p. To verify the prediction, we cloned the 3'-UTR of *AEG-1* into the luciferase reporter vector, and the control vector with the mutant 3'-UTR of *AEG-1* was also constructed. After co-transfection of the vector with miR-875-5p mimics into MHCC97-H cells, the luciferase activity was measured, showing about 55% reduction compared with the NC group. When the binding site of miR-875-5p in the 3'-UTR of *AEG-1* was mutated, the luciferase activity was rescued to the similar level with the control (*Figure 5B*). Furthermore, the endogenous mRNA and protein levels of *AEG-1* in MHCC97-H cells were both decreased after miR-875-5p mimic transfection confirmed by qRT-PCR and Western blot assays, respectively (*Figure 5C,D*). Moreover, the rescue assay had been performed to provide stronger evidence that miR-875-5p suppresses HCC proliferation and migration by inhibiting the expression of *AEG-1* as shown in *Figure S4*. Taken together, these results demonstrate that miR-875-5p targets the 3'-UTR of *AEG-1* to negatively regulate *AEG-1* expression.

Silencing of AEG-1 inhibits metastatic traits in HCC cells

The results above have demonstrated that miR-875-5p suppresses the metastatic traits in HCC cells and targets *AEG-1* gene to reduce its expression. To further verify these findings, we checked the performance of the HCC cells (MHCC97-H) after *AEG-1* knockdown using transwell migration and invasion. The results showed that knockdown of *AEG-1* decreased the number of migratory and invasive cells according to the crystal violet staining, with about 55% and 65% reduction in the migration and invasion activities (*Figure 6A,B*).

Furthermore, we also detected the effects of *AEG-1* knockdown on EMT both in MHCC97-H and HUH7 cells. The results showed that *AEG-1* knockdown decreased the expression of Vimentin and increased the expression of E-cadherin compared with the control analyzed by immunofluorescence analysis (*Figure 6C* and *Figure S5*). Taken together, these results demonstrate that the silencing

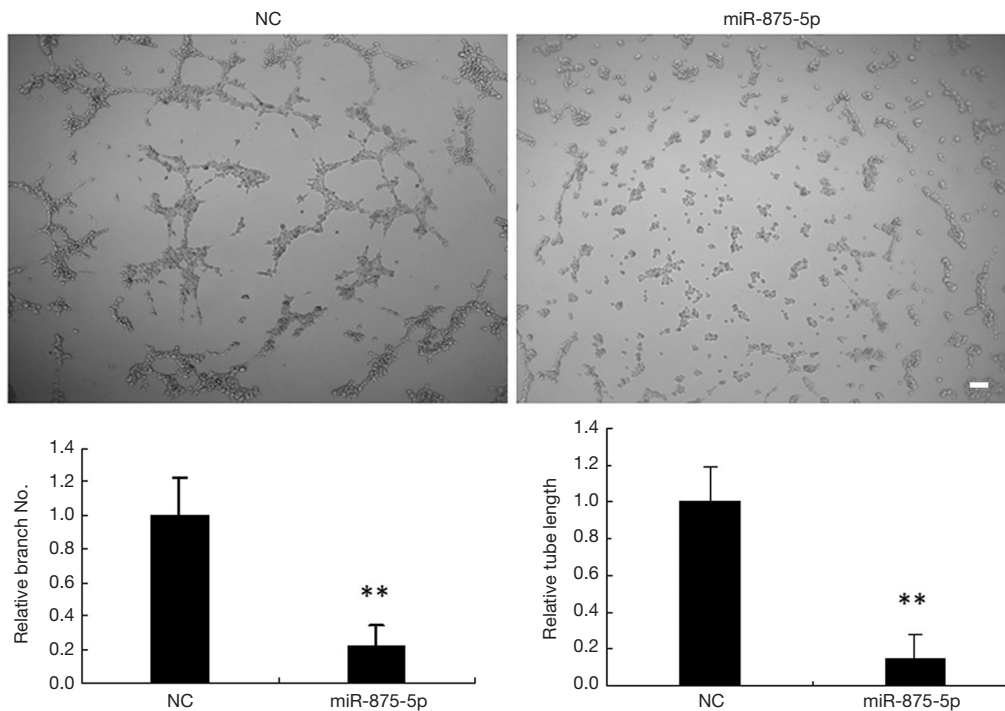


Figure 4 Effects of miR-875-5p over-expression on tubule elongation and branching formation in HUVEC cells. Bar =200 μ m. miR-875-5p mimic and control were transfected into MHCC97-H cells. The supernatants were collected at 72 h after transfection to add to the HUVEC cells, respectively. The tubule elongation and branching formation were analyzed afterwards. Visualize the cells using a light microscope. Take pictures of the images of the capillary network and count the tube lengths using the Scion image software. Visualize the cells using the light microscope. Take pictures of images of the capillary network (up) and count the tube lengths and branches (down) using the scion image software. **, indicates $P < 0.01$; NC, negative control; HUVEC, human umbilical vein endothelial cells.

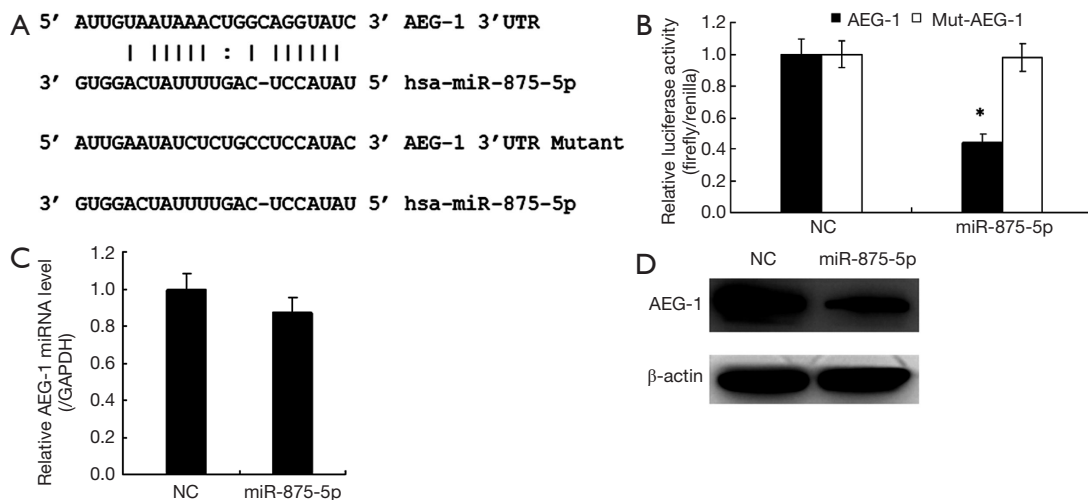


Figure 5 MiR-875-5p targets the 3'-UTR of *AEG-1* to decrease *AEG-1* expression. (A) The binding of miR-875-5p with the 3'-UTR of *AEG-1* and the mutant 3'-UTR predicted via miRNA.org algorithm; (B) the relative luciferase activity in MHCC97-H cells after co-transfection with miR-875-5p mimics and the indicated 3'-UTR- or mutant 3'-UTR-driven reporter plasmids. The expression levels of *AEG-1* in MHCC97-H cells after transfection with miR-875-5p mimics or NC were detected by real-time PCR (C) and Western blot (D), respectively. *, indicates $P < 0.05$; 3'-UTR, 3'-untranslated region; *AEG-1*, astrocyte elevated gene-1; NC, negative control.

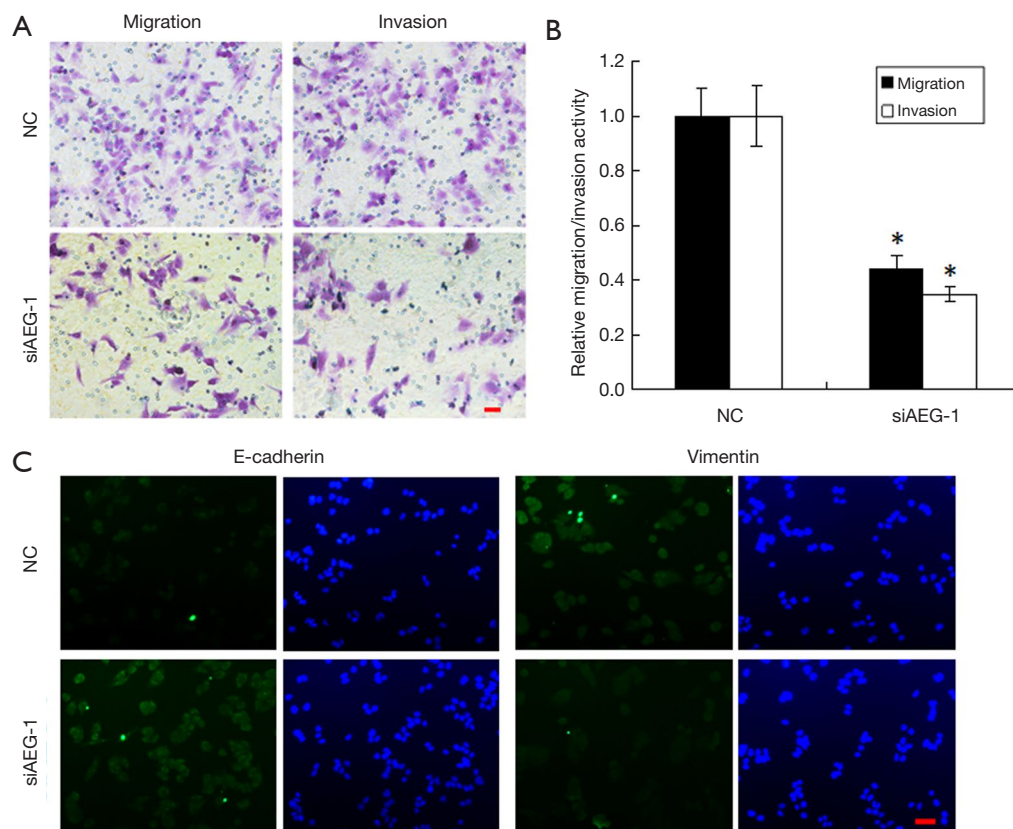


Figure 6 Knockdown of *AEG-1* attenuates the metastatic traits in MHCC97-H cells. (A) The crystal violet staining for the migratory and invasive cells after transfection of *AEG-1* siRNA or NC, and the relative migration/invasion activity was shown in (B). Bar = 50 μ m. (C) Immunofluorescence analysis for the expression of two EMT markers (E-cadherin and Vimentin, green) after *AEG-1* siRNA transfection. Nuclei were visualized by DAPI staining (blue). Bar = 100 μ m. *, indicates $P < 0.05$; *AEG-1*, astrocyte elevated gene-1; NC, negative control; EMT, epithelial-mesenchymal transition; DAPI, 2-(4-Aminidinophenyl)-6-indolecarbamide dihydrochloride.

of *AEG-1* inhibits metastatic traits in HCC cells.

The effects of *AEG-1* knockdown on cell proliferation and cell cycle of HCC cells

We further determined the effects of *AEG-1* knockdown on cell proliferation and cell cycle. According to the CCK8 assay result, the cell proliferation was decreased by approximately 45% (Figure 7A). To check the variation of cell cycle, FACS analysis of the cells after PI staining was performed. The proportion of the cells in G1 phase was obviously increased, while that in G2/M phase was decreased to some extent compared with control (Figure 7B). These findings indicate that knockdown of *AEG-1* is helpful to repress the cell proliferation of HCC cells and further confirm the function of miR-875-5p targeting *AEG-1*.

The effects of *AEG-1* knockdown on angiogenesis *in vitro* analyzed using HUVEC cells

To investigate whether *AEG-1* has effects on angiogenesis, we analyzed the branching formation and tubule elongation *in vitro* using HUVEC cells. Supernatants were collected at 72 h after *AEG-1* siRNA or control transfected into MHCC97-H cells to add to the HUVEC cells, respectively. HUVEC cells were seeded onto the matrigel-coated plates without angiogenic stimuli ahead of time. The tubule elongation and branching formation were analyzed 2 days culture afterwards. As shown in Figure 8, knockdown of *AEG-1* significantly inhibited the number of branching and the length of tubule compared to control, consistent with the effects of miR-875-5p over-expression, which further confirms that *AEG-1* is the target of miR-875-5p.

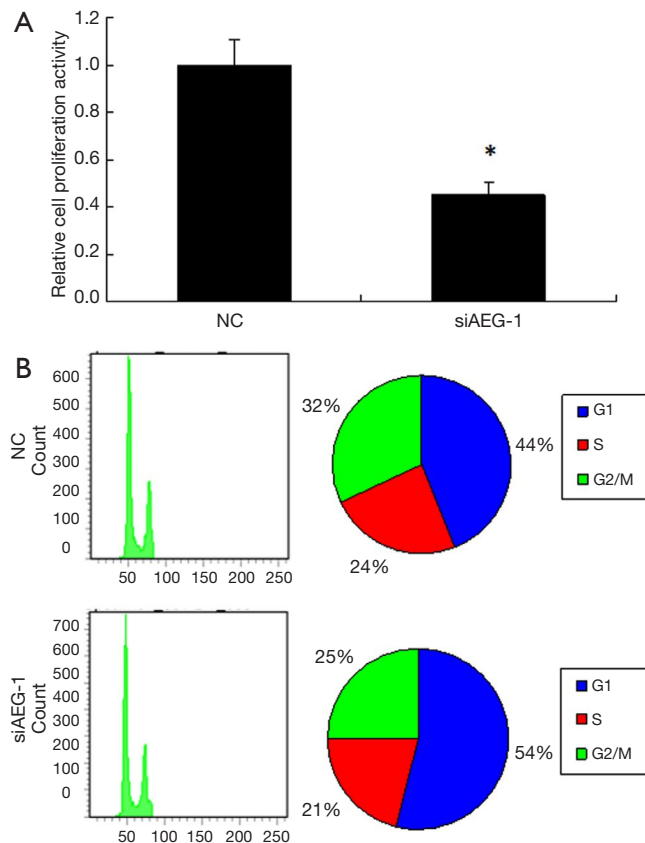


Figure 7 *AEG-1* knockdown has effects on MHCC97-H cell proliferation. *AEG-1* siRNA slightly induced G1 arrest and inhibits growth in MHCC97-H cells. (A) The viable cells were detected by CCK-8 assay 48 h after transfection with *AEG-1* siRNA and NC; (B) MHCC97-H cells were transfected with *AEG-1* siRNA and NC. The cells were collected and used for cell cycle analysis 48 h post transfection by flow cytometry after PI staining. The peak on the left indicates cells have diploid DNA content, the peak on the right indicates cells have tetraploid DNA content. *, indicates $P < 0.05$; *AEG-1*, astrocyte elevated gene-1; NC, negative control.

The expression of *AEG-1* in HCC tissues was elevated

According to the results above, the levels of miR-875-5p are decreased in HCC tissues, and *AEG-1* is a downstream target of miR-875-5p. Here, the expression of *AEG-1* in clinical tissues was further determined by immunohistochemical analysis. It was found that the expression of *AEG-1* in HCC tissues was relative higher than that in paracarcinoma tissues (Figure 9). Meanwhile, we also detected the expression of Glypican-3 (GPC-3), a marker for HCC. The level of GPC-3 in carcinoma tissues was higher than those in paracarcinoma tissues, similar

with the trends of *AEG-1*. These results indicate that HCC tissues express elevated level of *AEG-1*.

Discussion

HCC is a worldwide malignancy with no ideal targeted therapies. To achieve permanent cure of HCC, massive efforts are urgently needed to define the mechanisms of hepatocarcinogenesis, identify solid diagnostic biomarkers and develop effective therapeutic strategies (16,17).

Recent studies have reported that MiR-875-5p exerts tumor suppressor function by repressing EMT and downregulating EGFR in prostate cancer and colorectal carcinoma tissues, showing great potential as a target candidate for cancer therapy (14,15). However, the regulatory mechanism of miR-875-5p in HCCs largely unknown. In this study, we demonstrated that miR-875-5p was obviously decreased in HCC tissues compared with the matching adjacent non-tumor tissues (Figure 1). The expression patterns of miR-875-5p in various tissues may be different. Few studies indicated that the expression of miR-875-5p was up-regulated during tooth morphogenesis (18), suggesting that miR-875-5p may also be involved in other biological processes. Furthermore, over-expression of miR-875-5p negatively regulates the proliferation, migration and invasion of HCC cells, as well as angiogenesis *in vitro* modeled by HUVEC cells (Figures 2-4), which triggers an imagination that miR-875-5p may be a promising therapeutic target for HCC treatment. Similarly, the enforced expression of miR-199a in HCC cells leads to cell cycle arrest at G1 phase and reduces invasive capability (19). MiR-122 reduces migration and invasion *in vitro*, tumorigenesis and angiogenesis *in vivo*, and inhibited the local invasion in the liver of nude mice (20). In contrast, MiR-221 over-expression in HCC cells increases cell proliferation, migration and invasion capability, and enhances tumorigenesis in implanted mice (21,22)

The concrete promoting or suppressing activity of miRNAs in tumorigenesis largely depends on its downstream targets. In this study, we demonstrate that miR-875-5p could target the 3'-UTR of *AEG-1* gene to down-regulate its expression (Figure 5). *AEG-1* is a potentially crucial mediator of tumor malignancy and a key converging point of a complex network of oncogenic signaling pathways reported in recent years (23). Similar with the expression pattern in HCC (Figure 9), the levels of *AEG-1* are found to be elevated in breast carcinoma, melanoma and malignant glioma cell lines compared to their normal cellular

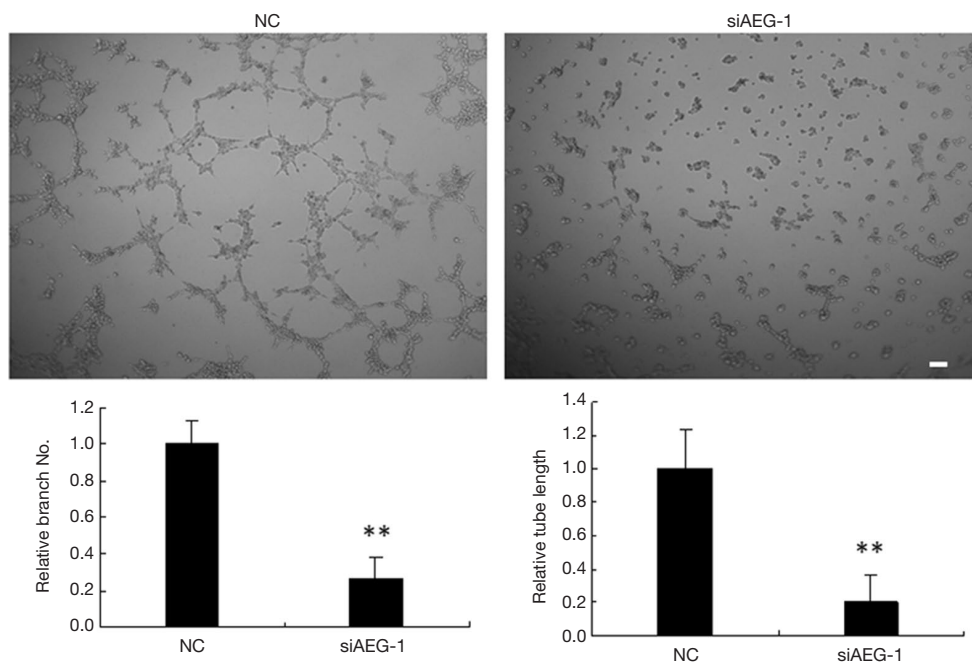


Figure 8 *AEG-1* knockdown affected the branching formation and tubule elongation in HUVEC cells. Bar =200 μ m. AEG siRNA and control were transfected into MHCC97-H cells. The supernatants were collected at 72 h after transfection to add to the HUVEC cells, respectively. The tubule elongation and branching formation were analyzed afterwards. Visualize the cells using a light microscope. Take pictures of the images of the capillary network and count the tube lengths using the Scion Image software. Visualize the cells using the light microscope. Take pictures of images of the capillary network (up) and count the tube lengths and branches (down) using the scion image software. **, indicates $P < 0.01$; AEG-1, astrocyte elevated gene-1; NC, negative control; HUVEC, human umbilical vein endothelial cells.

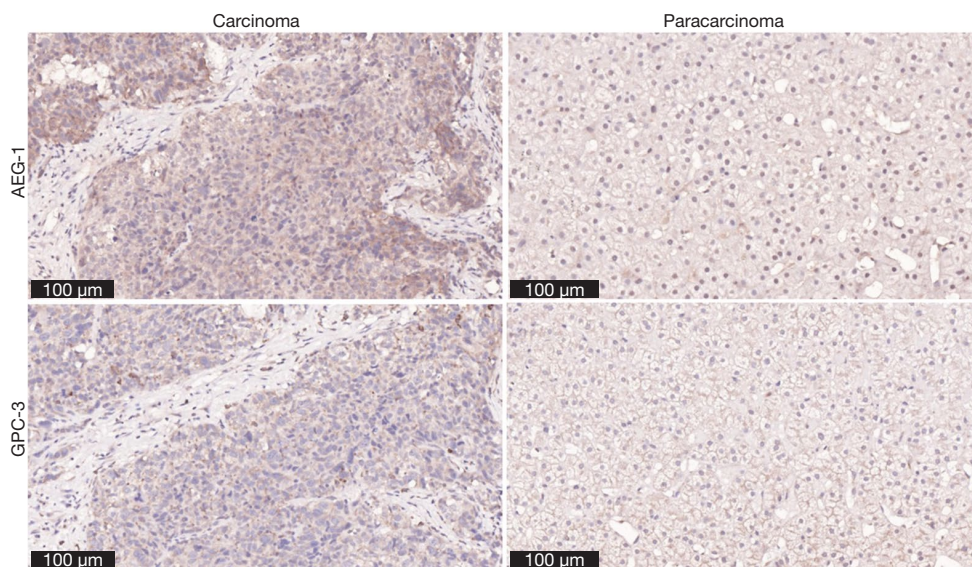


Figure 9 Immunohistochemistry analysis of the expression of *AEG-1* in metastatic hepatocellular carcinoma tissues. Representative immunohistochemical staining exhibited a strong staining of *AEG-1* in the GPC-3 high-expressing HCC tissues and weak staining of *AEG-1* in the GPC-3 low-expressing tumors. GPC-3 is a marker for hepatocellular carcinoma. Bar =100 μ m. AEG-1, astrocyte elevated gene-1; HCC, hepatocellular carcinoma.

counterparts (16). Here, the experimental results exhibited that *AEG-1* knockdown exerted the similar effects with miR-875-5p overexpression, with the reduced cell proliferation, migration, invasion and angiogenesis *in vitro*, and cell cycle arrest at G1 phase (Figures 6-8). Similarly, inhibition of *AEG-1* by siRNA significantly suppressed migration and invasion of malignant glioma cells and prostate cancer cells and lung metastasis of breast cancer cells *in vivo* (24).

A specific mRNA can be coordinately suppressed by several different miRNAs, and in turn one miRNA may have several targets (25). For example, except targeting *AEG-1* showed in this study, miR-875-5p can also target the 3'-UTR of EGFR mRNA in CRC cells (14). On the other hand, *AEG-1* can also be targeted by miR-375 in HCC cells (16). Therefore, the function networks of miRNAs and their targets are complex, and fully understanding of them is required.

Taken together, we give the evidence that miR-875-5p shows decreased levels in the HCC tissues and functions as a negative regulator in proliferation, migration, invasion and angiogenesis *in vitro* by targeting *AEG-1*. These results provide novel insights into the roles of miR-875-5p and its targets in HCC, and suggest an attractive direction for HCC target therapy.

Acknowledgments

Funding: This work was financially supported by the Beijing Natural Science Foundation [7174314], National Natural Science Foundation of China [81472328], National Science and Technology Support Program (2015BAI02B00), Capital Clinical Characteristics (Z171100001017063), Beijing municipal hospital scientific research project (PX2018057).

Footnote

Conflicts of Interest: All authors have completed the ICMJE uniform disclosure form (available at <http://dx.doi.org/10.21037/tcr.2018.01.22>). The authors have no conflicts of interest to declare.

Ethical Statement: The authors are accountable for all aspects of the work in ensuring that questions related to the accuracy or integrity of any part of the work are appropriately investigated and resolved. The study was conducted in accordance with the Declaration of Helsinki (as revised in 2013). Informed consent was obtained from all the patients and the present study was approved by the Ethics

Committee of the Capital Medical University in accordance with the Declaration of General hospital of Chinese PLA.

Open Access Statement: This is an Open Access article distributed in accordance with the Creative Commons Attribution-NonCommercial-NoDerivs 4.0 International License (CC BY-NC-ND 4.0), which permits the non-commercial replication and distribution of the article with the strict proviso that no changes or edits are made and the original work is properly cited (including links to both the formal publication through the relevant DOI and the license). See: <https://creativecommons.org/licenses/by-nc-nd/4.0/>.

References

1. Cancer Genome Atlas Research Network. Comprehensive and Integrative Genomic Characterization of Hepatocellular Carcinoma. *Cell* 2017;169:1327-41. e23.
2. Sia D, Villanueva A, Friedman SL, et al. Liver Cancer Cell of Origin, Molecular Class, and Effects on Patient Prognosis. *Gastroenterology* 2017;152:745-61.
3. Ghouri YA, Mian I, Rowe JH. Review of hepatocellular carcinoma: Epidemiology, etiology, and carcinogenesis. *J Carcinog* 2017;16:1.
4. Yu MW, Lin CL, Liu CJ, et al. Influence of Metabolic Risk Factors on Risk of Hepatocellular Carcinoma and Liver-Related Death in Men With Chronic Hepatitis B: A Large Cohort Study. *Gastroenterology* 2017;153:1006-17.e5.
5. Massagué J, Batlle E, Gomis RR. Understanding the molecular mechanisms driving metastasis. *Mol Oncol* 2017;11:3-4.
6. Sadhu SS, Wang S, Dachineni R, et al. In Vitro and In Vivo Antimetastatic Effect of Glutathione Disulfide Liposomes. *Cancer Growth Metastasis* 2017;10:1179064417695255.
7. Wang Y, Wang T, Sun Y, et al. Astrocyte elevated gene-1 promotes tumour growth and invasion by inducing EMT in oral squamous cell carcinoma. *Sci Rep* 2017;7:15447.
8. Cai Y, Yu X, Hu S, et al. A brief review on the mechanisms of miRNA regulation. *Genomics Proteomics Bioinformatics* 2009;7:147-54.
9. Esquela-Kerscher A, Slack FJ. Oncomirs - microRNAs with a role in cancer. *Nat Rev Cancer* 2006;6:259-69.
10. Zhu S, Wu H, Wu F, et al. MicroRNA-21 targets tumor suppressor genes in invasion and metastasis. *Cell Res* 2008;18:350-9.
11. Tavazoie SF, Alarcón C, Oskarsson T, et al. Endogenous human microRNAs that suppress breast cancer metastasis. *Nature* 2008;451:147-52.

12. Lin LL, Wang W, Hu Z, et al. Negative feedback of miR-29 family TET1 involves in hepatocellular cancer. *Med Oncol* 2014;31:291.
13. Li G, Zhang W, Gong L, et al. MicroRNA-125a-5p Inhibits Cell Proliferation and Induces Apoptosis in Hepatitis B Virus-Related Hepatocellular Carcinoma by Downregulation of ErbB3. *Oncol Res* 2017. [Epub ahead of print].
14. El Bezawy R, Cominetti D, Fenderico N, et al. miR-875-5p counteracts epithelial-to-mesenchymal transition and enhances radiation response in prostate cancer through repression of the EGFR-ZEB1 axis. *Cancer Lett* 2017;395:53-62.
15. Zhang T, Cai X, Li Q, et al. Hsa-miR-875-5p exerts tumor suppressor function through down-regulation of EGFR in colorectal carcinoma (CRC). *Oncotarget* 2016;7:42225-40.
16. He XX, Chang Y, Meng FY, et al. MicroRNA-375 targets AEG-1 in hepatocellular carcinoma and suppresses liver cancer cell growth in vitro and in vivo. *Oncogene* 2012;31:3357-69.
17. Santamaría E, Muñoz J, Fernández-Irigoyen J, et al. Toward the discovery of new biomarkers of hepatocellular carcinoma by proteomics. *Liver Int* 2007;27:163-73.
18. Michon F, Tummers M, Kyrrönen M, et al. Tooth morphogenesis and ameloblast differentiation are regulated by micro-RNAs. *Dev Biol* 2010;340:355-68.
19. Jia XQ, Cheng HQ, Qian X, et al. Lentivirus-mediated overexpression of microRNA-199a inhibits cell proliferation of human hepatocellular carcinoma. *Cell Biochem Biophys* 2012;62:237-44.
20. Bai S, Nasser MW, Wang B, et al. MicroRNA-122 inhibits tumorigenic properties of hepatocellular carcinoma cells and sensitizes these cells to sorafenib. *J Biol Chem* 2009;284:32015-27.
21. Fornari F, Gramantieri L, Ferracin M, et al. MiR-221 controls CDKN1C/p57 and CDKN1B/p27 expression in human hepatocellular carcinoma. *Oncogene* 2008;27:5651-61.
22. Pineau P, Volinia S, McJunkin K, et al. miR-221 overexpression contributes to liver tumorigenesis. *Proc Natl Acad Sci U S A* 2010;107:264-9.
23. Emdad L, Sarkar D, Su ZZ, et al. Astrocyte elevated gene-1: recent insights into a novel gene involved in tumor progression, metastasis and neurodegeneration. *Pharmacol Ther* 2007;114:155-70.
24. Emdad L, Lee SG, Su ZZ, et al. Astrocyte elevated gene-1 (AEG-1) functions as an oncogene and regulates angiogenesis. *Proc Natl Acad Sci U S A* 2009;106:21300-5.
25. Callegari E, Elamin BK, Sabbioni S, et al. Role of microRNAs in hepatocellular carcinoma: a clinical perspective. *Onco Targets Ther* 2013;6:1167-78.

Cite this article as: Hu C, Cui S, Zheng J, Yin T, Lv J, Long J, Zhang W, Wang X, Sheng S, Zhang H, Sun Y, Wang H, Li C. MiR-875-5p inhibits hepatocellular carcinoma cell proliferation and migration by repressing *astrocyte elevated gene-1 (AEG-1)* expression. *Transl Cancer Res* 2018;7(1):158-169. doi: 10.21037/tcr.2018.01.22

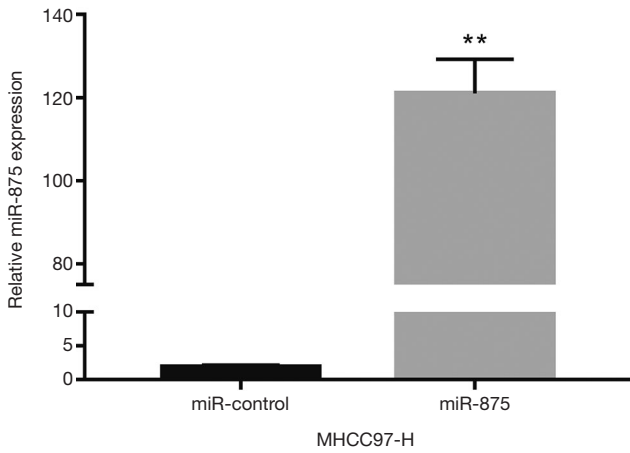


Figure S1 The Relative Expression of miR-875-5p in MHCC97-H cells transfected with miR-875-5p mimic or control. qRT-PCR analysis determined that miR-875-5p expression in miR-875-5p-mimic-transfected cells was significantly higher than control. **, indicates $P < 0.01$. qRT-PCR, quantitative real-time polymerase chain reaction.

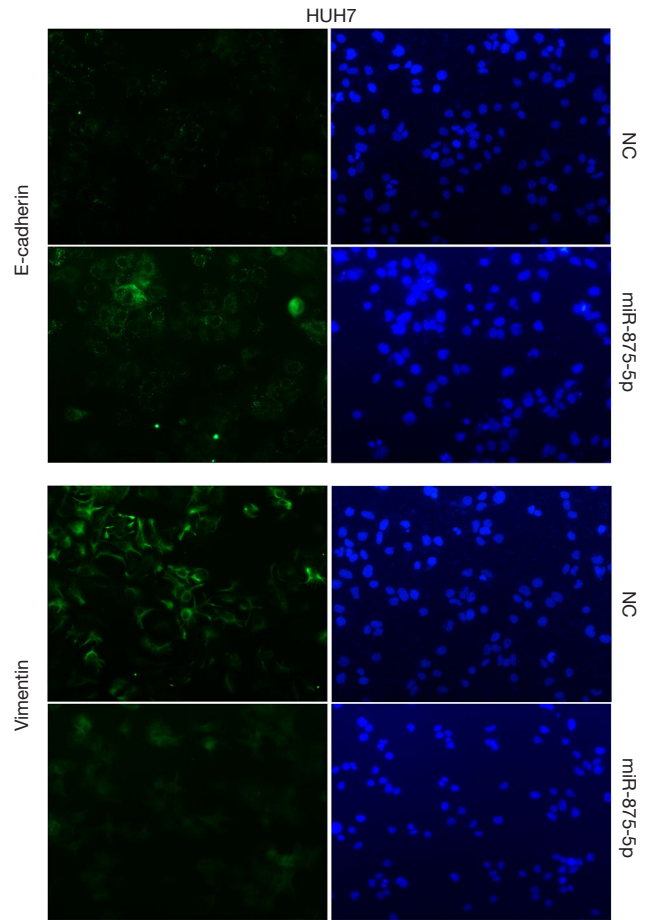


Figure S2 Analysis of immunofluorescence for EMT markers in HUH7 cells. Immunofluorescence for the expression of two EMT markers was analyzed after miR-875-5p mimics transfection in HUH7. HUH7 cells were stained for E-cadherin (green) and Vimentin (green) respectively and DAPI for visualization of the nucleus (blue). The representative staining shows a 40 \times magnification; Bar =100 μ m. The representative staining shows a 40 \times magnification. Bar =100 μ m. EMT, epithelial-mesenchymal transition; NC, negative control; DAPI, 2-(4-Amidinophenyl)-6-indolecarbamide dihydrochloride.

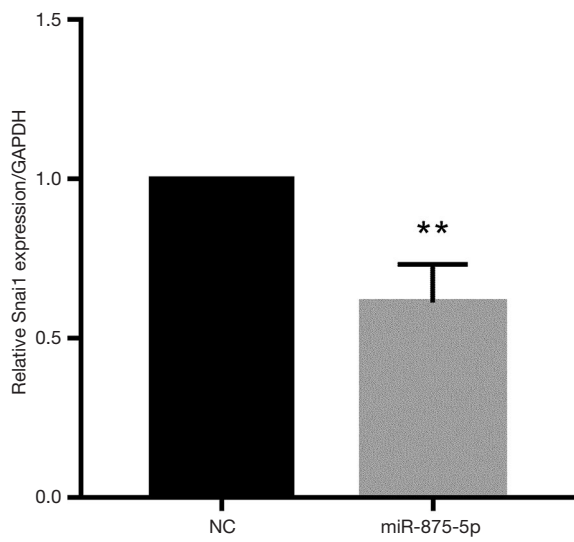


Figure S3 The relative expression of snail in MHCC97-H cells transfected with miR-875-5p mimic or control. qRT-PCR analysis revealed that the expression of snail, another EMT marker in miR-875-5p-mimic-transfected cells was reduced obviously than control. **, indicates $P < 0.01$; qRT-PCR, quantitative real-time polymerase chain reaction; EMT, epithelial-mesenchymal transition.

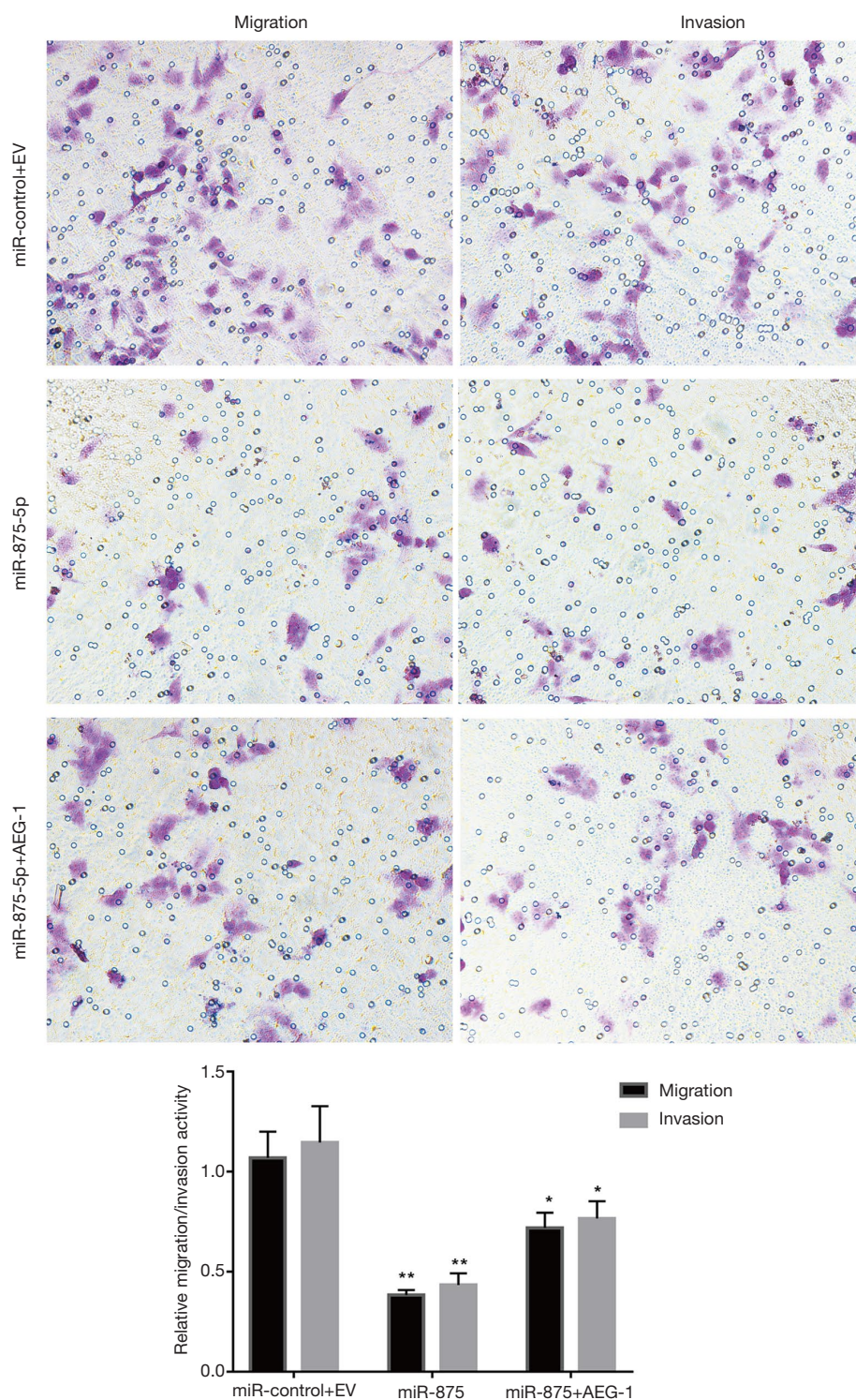


Figure S4 *AEG-1* over-expression rescued the MiR-875-5p-induced metastatic inhibition in MHCC97-H cells. Cell migration and invasion as assessed by transwell assays were inhibited by overexpression of miR-875-5p in MHCC97-H cells. *AEG-1* over-expression could partially rescue the phenotype induced by miR-875-5p mimic. The crystal violet staining for the migratory and invasive cells was assessed after transfection of miR-875-5p mimics, miR-875-5p mimics and *AEG1* overexpression and the NC. The relative migration/invasion activity was shown in the bottom. Bar = 50 μ m. *, indicates $P < 0.05$; **, indicates $P < 0.01$. *AEG-1*, astrocyte elevated gene-1; NC, negative control.

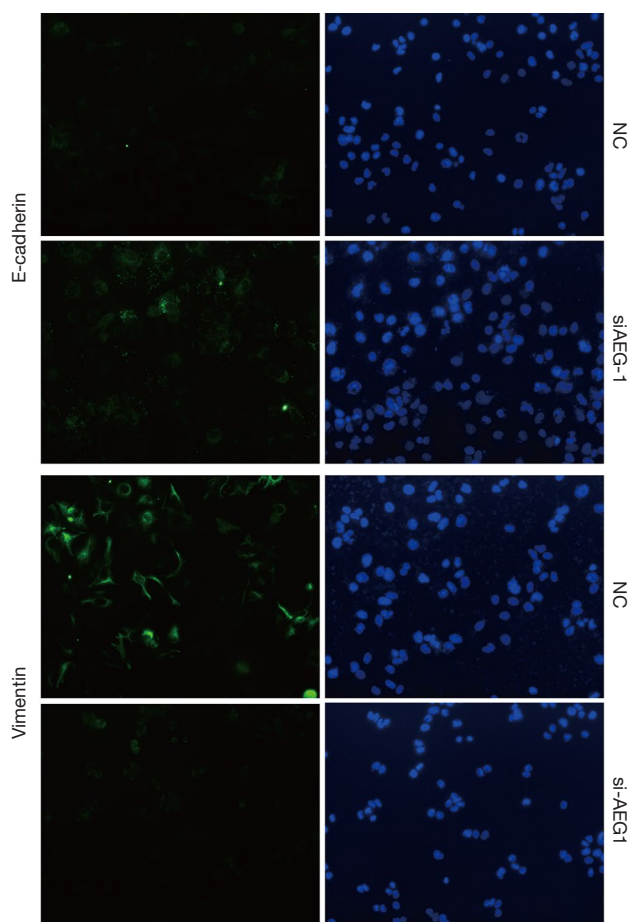


Figure S5 Immunofluorescence for the expression of two EMT markers was analyzed in *AEG-1*-knockdown HUH7 cells. HUH7 cells were stained for E-cadherin (green) and Vimentin (green) respectively and DAPI for visualization of the nucleus (blue). The representative staining shows a 40× magnification. Bar =100 μm. EMT, epithelial-mesenchymal transition; AEG-1, astrocyte elevated gene-1; NC, negative control; DAPI, 2-(4-Amidinophenyl)-6-indolecarbamide dihydrochloride.